Biophysical Chemistry 28 (1987) 93–99
Elsevier

BPC 01186

Motion of proton in double-well potential

Its possible role in the process of vision

Oscar J. Riveros

Department of Chemistry, Purdue University, W. Lafayette, IN 47907, U.S.A.

Received 5 May 1987
Accepted 16 July 1987

Proton transfer; Vision; Quantum-mechanical calculation

A quantum-mechanical model that allows direct calculation of the rate of proton transfer with possible application to the early events in vision is presented. The rate is obtained in closed form in the linear-response approximation in terms of four parameters. The model permits a simple calculation of these parameters and shows modest agreement with the experimentally determined rate constant.

1. Introduction

Proton transfer has for many years been the subject of active research in chemistry [1,2]. Its possible role in the early events of vision continues to attract the attention of biochemists and biophysicists as well [3–5]. The process is initiated by the absorption of light by the 11-*cis*-retinal chromophore of rhodopsin; the electronically excited rhodopsin then rapidly decays to produce an intermediate species called bathorhodopsin [6]. The precise mechanism of this primary process remains a matter of considerable controversy. The most common explanation has been that light causes the double bond at C-11 to isomerize from the *cis* to *trans* configuration [7–10]. Picosecond measurements [8] and molecular-dynamic calculations [11,12] indicate that this process may indeed be very rapid. On the other hand, time-resolved picosecond experiments performed by Peters et al. [13] suggest that the rate-limiting step governing the production of bathorhodopsin involves proton translocation to the Schiff-base nitrogen of retinal in the excited state of rhodopsin. Their suggestion is based on the strong deuterium-isotope effect observed in the rate of formation of bathorhodopsin. Moreover, the strong non-Arrhenius thermal dependence of the observed rate constant is indicative of quantum-mechanical tunneling.

A variety of models have detailed mechanisms describing the molecular events which follow excitation of rhodopsin and lead to the formation of bathorhodopsin [9–11,14,15]. However, there does not seem to be sufficient information available as yet on the structure of rhodopsin to permit an unambiguous interpretation of existing kinetic data.

Sarai et al. [16] have performed CNDO/2 calculations for a model of rhodopsin consisting of the retinal chromophore hydrogen bonded through the Schiff-base nitrogen to lysine, the entire complex being isolated. The calculated potential-energy curves for the motion of the Schiff-base proton along a line between the two

Correspondence (present) address: O.J. Riveros, Indiana University School of Medicine, 635 Barnhill Drive, Indianapolis, IN 46223, U.S.A.

fixed nitrogens indicate that the proton moves in an unsymmetric double-minimum potential well at any conformation about the C_{11}–C_{12} bond ranging from all-*trans* to all-*cis* (see also ref. 5). The results of their calculations suggest that proton transfer takes place in the excited state of rhodopsin in a concerted way with isomerization during the early stages of the visual process. However, they provide no quantitative expression for the rate constants associated with any of the elementary steps.

In this article, we present a quantum-mechanical two-state model calculation for the rate of proton transfer, W_{10} which may be relevant to the early events of vision. The transfer rate can be cast in closed form in terms of four parameters using Fong's prescription for radiationless relaxation in solids [17,18]. This requires that we first determine a set of unperturbed (zero-order) energy eigenstates of the system. In our model, we shall find these states by invoking the double adiabatic approximation [19], in which the motion of the electrons is separated from that of all the nuclei and, in turn, the motion of the proton is separated from that of the heavier nuclei. The significant rate parameters are as follows: $\Delta\epsilon_{10}$, the difference between the minima of the potential-energy surfaces corresponding to the ground ($i = 0$) and first excited ($i = 1$) states of the proton; ω_m, the normal mode frequency; g_m, which is proportional to the shift in the equilibrium position of the normal mode and C_{10}, which is proportional to the strength of the coupling between the protonic states.

In the present treatment transitions between the zero-order protonic states are induced by the nuclear kinetic energy operator. The basic assumptions underlying this approach are: (1) the heavy-nuclear motion is harmonic; (2) only a single mode mediates the process and (3) the normal modes in the initial and final states are parallel. In particular, under these restrictions, the rate may be represented by [17]:

$$W_{10} = (2\pi)^{1/2}\hbar^{-2}|C_{10}|^2\omega_m^{-1}\sum_\nu \lambda_\nu (p_m-\nu)^{-1/2} \times\exp\left[-g_m^2(2n_m+1)\right] \times\exp\left\{-(p_m-\nu)\left[\ln\left((p_m-\nu)/g_m^2(n_m+1)\right)-1\right]\right\}, \tag{1}$$

where

$$C_{10} = -\left(\hbar^3\omega_m/2\right)^{1/2}\Delta\epsilon_{10}^{-1}V_{10} \tag{2a}$$

and

$$\Delta\epsilon_{10} = \epsilon_1(0)-\epsilon_0(0) \tag{2b}$$

The term V_{10} is shown below (eq. 19) and the remaining quantities p_m, λ_ν, g_m and n_m are given explicitly in ref. 17. In deriving eq. 1 we have also assumed that only a single mode, Q_m, of fixed frequency mediates the process. Furthermore, this expression is valid only if the following relations between the parameters hold:

$$\rho = (\Delta\epsilon_{10}-\hbar\omega_m)/g^2\hbar\omega_m \gg 1 \tag{3a}$$

$$\rho\,\sinh(\beta\hbar\omega_m/2) \gg 1 \tag{3b}$$

To evaluate eq. 1 we must determine the rate parameters $\Delta\epsilon_{10}$, C_{10}, ω_m and g_m. We do this by introducing a crude model for proton translocation in section 2. This model, however, does not take explicit account of the role of isomerization. This restriction is adopted in order to simplify the subsequent theoretical developments.

2. Model for proton motion in double-well potential

For a given potential the motion of the proton can be determined by the Schrödinger equation

$$\left\{-\left(\hbar^2/2m_h\right)\nabla_r^2 + V(\boldsymbol{r},\boldsymbol{R})\right\}\phi_i(\boldsymbol{r},\boldsymbol{R}) = \epsilon_i(\boldsymbol{R})\phi_i(\boldsymbol{r},\boldsymbol{R}) \tag{4}$$

where r denotes the proton's coordinate and $\boldsymbol{R}$ the collection of heavy-nuclear coordinates. $V(\boldsymbol{r},\boldsymbol{R})$ is the full adiabatic potential-energy surface associated with the relevant electronic

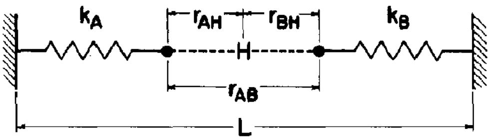

Fig. 1. One-dimensional model of the chromophore molecule of rhodopsin.

state. $\phi_i(\boldsymbol{r},\boldsymbol{R})$ is the Born-Oppenheimer protonic energy eigenstate and $\epsilon_i(\boldsymbol{R})$ its corresponding eigenvalue. ϵ_i defines the effective potential seen by the heavy nuclei.

In this model, the proton moves along a line between atoms (or rigid groups) A and B (see fig. 1). The groups A and B are, in turn, bonded to the remainder of the opsin matrix. Further, we assume that the proton experiences a double-well potential, which we take to be a sum of two Morse potentials centered on A and B (see fig. 1):

$$V = U_{\mathrm{AH}} + U_{\mathrm{AH}} \tag{5}$$

$$U_{\mathrm{AH}} = D_{\mathrm{AH}}\left\{1 - \exp\left[-\left(r_{\mathrm{AH}} - r_{\mathrm{AH}}^0\right)/d_{\mathrm{AB}}\right]\right\}^2 \tag{6a}$$

$$U_{\mathrm{BH}} = D_{\mathrm{BH}}\left\{1 - \exp\left[-\left(r_{\mathrm{BH}} - r_{\mathrm{BH}}^0\right)/d_{\mathrm{AH}}\right]\right\}^2 \tag{6b}$$

Substituting eqs. 5 and 6 into eq. 4, we obtain a one-dimensional Schrödinger equation for the Born-Oppenheimer protonic wavefunctions parametric in the single distance r_{AB} (see fig. 1). This equation was solved by the standard three-point finite-difference scheme [20–22]. The finite-difference mesh extended from −1.74 to 1.74 Å, where the position of the proton was referred to the geometric center of A and B. At the end points the potential was less than 10^5 cm^{-1} in all cases, which is sufficiently high that the protonic wavefunction can be well approximated by zero, as required by the finite-difference method.

Considerable trial and error was required in order to arrive at a set of Morse potential parameters that yielded rate parameters in approximate agreement with those determined from experiment. As an initial 'guess' we fitted the two Morse potentials to the potential-energy curves obtained by Sarai et al. [16] using the CNDO method. For simplicity, we set $r_{\mathrm{AH}}^0 = r_{\mathrm{BH}}^0$ and $d_{\mathrm{AH}} = d_{\mathrm{BH}}$, thus reducing the number of Morse parameters to four. These results are listed in table 1. Fig. 2 shows plots of the lowest two eigenfunctions. By changing the A–B distance and then recalculating the eigenvalues for this new distance, we generated a plot of ϵ_i vs. r_{AB} (fig. 3). From these curves the value for the parameter $\Delta\epsilon_{10}$ is obtained simply as the vertical difference between the minima.

Table 1

Parameters of the model

$D_{\mathrm{AH}} = 9000$ cm^{-1}
$D_{\mathrm{BH}} = 8500$ cm^{-1}
$d_{\mathrm{AH}} = d_{\mathrm{BH}} = 0.65$ Å
$r_{\mathrm{AH}}^0 = r_{\mathrm{BH}}^0 = 0.91$ Å
$m_{\mathrm{A}} = m_{\mathrm{B}} = m = 800$ a.m.u.
$K_{\mathrm{A}} = K_{\mathrm{B}} = K = 1.0 \times 10^4$ dyn cm^{-1}
$r_{\mathrm{A}}^0 = r_{\mathrm{B}}^0 = 0.96$ Å
$L = 5.22$ Å

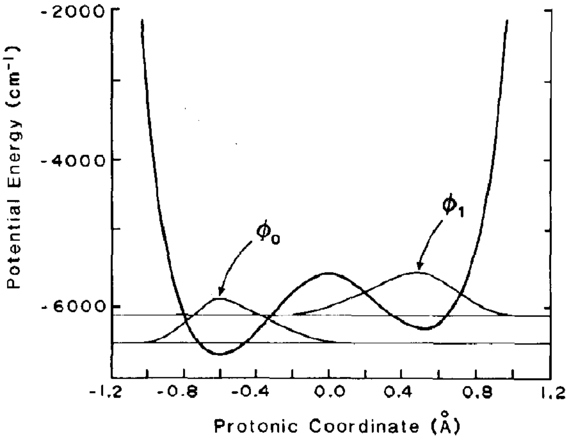

Fig. 2. Plot of model potential corresponding to the parameters in table 1. Also shown are the lowest two eigenvalues and corresponding eigenfunctions. $r_{\mathrm{AB}} = 3.30$ Å.

The normal modes of the heavy nuclei were determined within the harmonic approximation. Only the colinear motion of A and B is explicitly taken into account, the remainder of the system being treated as a rigid body of infinite mass. The force constant and equilibrium distance for the A–B interaction are found by fitting ϵ_i (r_{AB}) to a parabola

$$\epsilon_i(r_{\mathrm{AB}}) = K_i\left(r_{\mathrm{AB}} - r_i^0\right)^2/2 + V_{i0} \quad i = 0, 1 \tag{7}$$

using three points about the minimum [23]. The specific values of K_0 and r_i^0 corresponding to the chosen potential parameters are listed in table 2. The masses $(m_{\mathrm{A}}, m_{\mathrm{B}})$ of the groups A and B and the force constants $(K_{\mathrm{A}}, K_{\mathrm{B}})$ and equilibrium separations $(r_{\mathrm{A}}^0, r_{\mathrm{B}}^0)$ associated with the bonds between A and B and the remainder of the system are additional parameters of the model and are

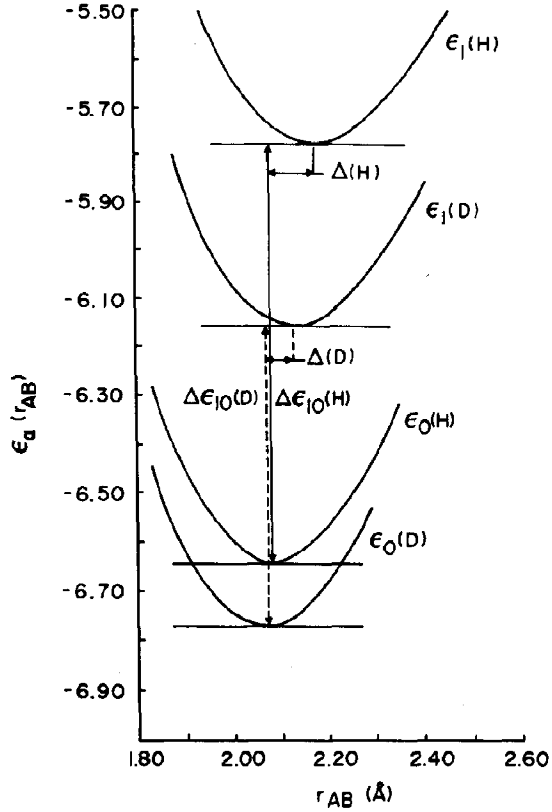

Fig. 3. Plots of adiabatic potential-energy surfaces for heavy-nuclear motion. Energy is measured in units of 1850 cm^{-1}.

assumed not to depend upon the protonic state i. They are entered in the model with typical values (see below).

When the proton is in the ground state ($i = 0$), the potential energy governing the heavy-nuclear motion can be written

$$U_0(r_A, r_B) = \tfrac{1}{2}K_A(r_A - r_A^0)^2 + \tfrac{1}{2}K_0(r_B - r_A - r_{AB}^0)^2 + \tfrac{1}{2}K_B(L - r_B - r_B^0)^2 \tag{8}$$

Table 2

Computed parameters for the model

	K_0 (dyn cm^{-1})	r_0^0 (Å)	r_1^0 (Å)	Δ (Å)	r_{AB}^0 (Å)
Hydrogen	5.4×10^4	2.08	2.18	0.10	3.30
Deuterium	5.4×10^4	2.07	2.14	0.07	3.30

where L is the total distance between the ends of the effective protein cavity containing the groups (see fig. 1). We assume that L remains fixed. Defining Δr_A and Δr_B as displacements of A and B from their respective equilibrium positions, we can rewrite eq. 8 as

$$U_0(\Delta r_A, \Delta r_B) = \tfrac{1}{2}K_A\,\Delta r_A^2 + \tfrac{1}{2}K_0(\Delta r_A - \Delta r_B)^2 + \tfrac{1}{2}K_B\,\Delta r_B^2 \tag{9}$$

The normal modes Q_1 and Q_2 are given in terms of the displacements as [24]:

$$Q_1 = M_A^{1/2}\cos\alpha\,\Delta r_A + m_B^{1/2}\sin\alpha\,\Delta r_B \tag{10a}$$

$$Q_2 = m_B^{1/2}\cos\alpha\,\Delta r_B - m_A^{1/2}\sin\alpha\,\Delta r_A \tag{10b}$$

where

$$\tan 2\alpha = 2(m_A m_B)^{1/2}K_0/[m_A K_A - m_B K_B + (m_A - m_B)K_0] \tag{11}$$

In the normal-mode representation, the potential energy for the heavy motion (with the proton in the ground state $i = 0$) is given by

$$U_0(Q_1, Q_2) = \tfrac{1}{2}\omega_1^2 Q_1^2 + \tfrac{1}{2}\omega_2^2 Q_2^2 \tag{12}$$

When the proton is in the first excited state, this becomes

$$U_1(Q_1, Q_2) = \tfrac{1}{2}\omega_1^2(Q_1 - \Delta Q_1)^2 + \tfrac{1}{2}\omega_2^2(Q_2 - \Delta Q_2)^2 + \text{const.} \tag{13}$$

with

$$\Delta Q_1 = [m_A^{1/2}\cos\alpha\,\Delta_A + m_B^{1/2}\sin\alpha\,\Delta_B] \tag{14a}$$

$$\Delta Q_2 = [m_B^{1/2}\cos\alpha\,\Delta_B - m_A^{1/2}\sin\alpha\,\Delta_A] \tag{14b}$$

The displacements of the equilibrium positions of A and B are

$$\Delta_A = -K_0 K_B\,\Delta/[(K_A + K_0)(K_0 + K_B) - K_0^2] \tag{15a}$$

$$\Delta_B = K_A K_0\,\Delta/[(K_A + K_0)(K_0 + K_B) - K_0^2] \tag{15b}$$

where

$$\Delta \equiv (r_1^0 - r_0^0) \tag{16}$$

is the shift in the equilibrium separation of A and B (see fig. 3, where Δ is shown as the horizontal displacement of the minimum).

For simplicity, we set $K_A = K_B = K$ and $m_A = m_B = m$ in the above equations. Then, substituting into eqs. 10 and 11, we obtain:

$$Q_1 = (m/2)^{1/2}[\Delta r_A + \Delta r_B];\ \omega_1 = (K/m)^{1/2} \tag{17a}$$

$$Q_2 = (m/2)^{1/2}[-\Delta r_A + \Delta r_B];\quad \omega_2 = [(2K_0 + K)/m]^{1/2} \tag{17b}$$

where Δr_x represents the atomic displacement. The mode Q_1 corresponds to the 'external' motion of both A and B in concert; Q_2 is the 'internal' vibration of AB as a 'diatomic molecule'. The reduced displacement g_1 vanishes and

$$g_2^2 = [m/(K + 2K_0)]^{1/2} K_0^2\, \Delta^2 / [\hbar (K + 2K_0)] \tag{18}$$

where Δ is the shift in the equilibrium separation (r_{AB}^0) between A and B.

Taking the effective mass of the groups A and B to be $m \approx 800$ a.m.u. and the effective force constant to be $K \approx 10^4$ dyn cm^{-1}, we compute $\omega_2 \approx 50$ cm^{-1} from eq. 17b. Then, using the values of Δ (see table 3) obtained from the plots of fig. 3, we calculate from eq. 18 the values for the displacements g_2 (given in table 3). Note that the difference between the g_2 for ^{1}H and that for ^{2}H arises solely from the factor Δ^2 in eq. 18 in this case, since K_0 shows no isotope effect.

In order to estimate the parameter C_{10}, we need to compute the matrix element

$$V_{10} = \int \mathrm{d}r\, \phi_1^*(r; r_{AB})(\partial V/\partial r_{AB})\phi_0(r; r_{AB})\, |_{r_{AB} = r_{AB}^0} \tag{19}$$

Table 3

Computed parameters from the model

Isotope	ω_2 (cm^{-1})	$\lvert C_{10}\rvert^2$ (erg^2)	g_2	$\Delta\epsilon_{10}$ (cm^{-1})
Hydrogen	50	5.4 (−29)	1.58	1590
Deuterium	50	6.31 (−30)	1.11	1100

This integral is approximated by means of the extended Simpson's rule [20], with the gradient $\partial V/\partial r_{AB}$ evaluated in closed form from eqs. 5 and 6. Once V_{10} is obtained a simple relation leads to the desired parameter C_{10} (see eq. 2). The results of these model calculations are summarized in table 3.

3. Application to early events in vision

This model was used to interpret the thermal behavior of the experimentally determined rate constant [13]. However, the insufficient amount of experimental data and the large errors associated with each point render any precise correlation between theory and experiment impracticable. We decided to resolve this conflict by adopting a semi-empirical approach and simply fitted the observed rate to eq. 1. Two different sets of parameters were obtained. The results of this fitting are presented in table 4.

Comparison between tables 3 and 4 reveals only semiquantitative agreement. The frequency ω_2 is the only parameter that remains unchanged under deuterium substitution. The ^{2}H remaining parameters show a clear isotope dependence: $\Delta\epsilon_{10}(^2\mathrm{H})$ is about 25% less than $\Delta\epsilon_{10}$ (^{1}H); $|C_{10}|^2(^2\mathrm{H})$ is 1–3 orders of magnitude less than $|C_{10}|^2(^1\mathrm{H})$; $g_2(^2\mathrm{H})$ is less than $g_2(^1\mathrm{H})$. The reason that the model predicts no isotopic frequency shift is clear from eq. 17b. The effective bond force constant K_0 is unaltered by deuteration (see table 2) and K and m are fixed by assumption. However, if hydrogens other than the translocating proton are exchanged for deuterons, the effec-

Table 4

Results of fitting eq. 1 to experimental rate data [13]

Fitting	Isotope	ω_m (cm^{-1})	$\lvert C_{10}\rvert^2$ (erg^2)	g_m	$\Delta\epsilon_{10}$ (cm^{-1})	ρ
1	^{1}H	38.2	0.11 (−24) [a]	2.68	1200	4.1
	^{2}H	34.3	6.60 (−27)	2.58	930	3.8
2	^{1}H	26.9	1.94 (−26)	0.77	277	13.9
	^{2}H	23.2	3.34 (−28)	0.64	197	15.8

[a] Numbers in parentheses indicate powers of ten by which entry should be multiplied.

tive mass (m) of groups A and B might well increase upon deuteration. To realize the experimental decrease of 8.6% in ω_2 would require an increase of about 150 a.m.u. for groups of mass 800.

4. Discussion

The model proposed here could be used to support the idea of proton translocation to the Schiff base as one of the primary steps of vision. However, it can also be used to advocate the idea of proton transfer within the protein (opsin matrix) as suggested by various authors [5,9,15]. We cannot decide between these two alternatives before a more detailed knowledge of the potential-energy surface for the protonic motion becomes available. For example, the presence of the protein environment may change the potential-energy barrier or the hydrogen-bond distance. This may result in significant changes in some of the rate parameters.

Another interesting point apparent in table 3 is the presence of a low-frequency vibration mediating the proton translocation (also present in table 4). This mode could be associated with a slow vibrational motion of either all or a large portion of the opsin matrix, since the chromophore molecule is embedded in this protein. While this result is specific for this model it supports the observation that low-frequency motions play an active role in important biological functions [25,26].

The present model calculation did not take account of anharmonicity effects. We noticed, however, that for larger values of r_{AB}, the heavy-nuclear energy curves (fig. 3) start departing from simple quadratic behavior. In this case, the harmonic approximation invoked while arriving at eq. 1 is valid only for small values of the displacement Δ. This situation may indeed prevail here, since the values of Δ computed from the model are relatively small (see table 3). In any event, the model presented here, although subject to anharmonic corrections in its present form, allows us to estimate reasonable orders of magnitudes and trends for the molecular parameters in a problem of prevailing interest.

Acknowledgements

I wish to thank Professor Dennis J. Diestler for innumerable discussions and insightful comments on this model calculation. I also wish to thank Professor William McD. Armstrong for his kind hospitality while the last version of this paper was being written.

References

1 G. Zundel, in: The hydrogen bond, vol. 2, eds. P. Schuster, G. Zundel and C. Sandorfy (North-Holland, Amsterdam, 1976) p. 683.

2 R.P. Bell, in: The tunnel effect in chemistry (Chapman and Hall, London, 1980) p. 1.

3 B. Honig, Annu. Rev. Phys. Chem. 29 (1978) 31; M.L. Applebury, Photochem. Photobiol. 32 (1980) 425; R.R. Birge, Annu. Rev. Biophys. Bioeng. 10 (1981) 315; R.R. Birge, L.P. Murray, B.M. Pierce, H. Akita, V. Balogh-Nahir, L.A. Findsen and K. Nakanishi, Proc. Natl. Acad. Sci. U.S.A. 82 (1985) 4117.

4 R. Lewis, Science 227 (1985) 500.

5 J.M. Leclercq, P. Dupuis and C. Sandorfy, Croat. Chem. Acta 55 (1982) 105; J.M. Leclercq and C. Sandorfy, J. Raman Spectrosc. 14 (1983) 358; C. Sandorfy and D. Vocelle, Can. J. Chem. 64 (1986) 2251.

6 G.E. Busch, M.L. Applebury, A.A. Lamola and P.M. Rentzepis, Proc. Natl. Acad. Sci. U.S.A. 69 (1972) 2803.

7 T. Yoshizawa and G. Wald, Nature 197 (1963) 1279.

8 B.H. Green, T.G. Monger, R.R. Alfano, B. Aton and R.H. Callender, Nature 269 (1977) 179.

9 T. Rosenfeld, B. Honig, M. Ottolenghi, J. Hurley and T.G. Ebrey, Pure Appl. Chem. 49 (1977) 341.

10 B. Honig, T. Ebrey, R.H. Callender, U. Dinur and M. Ottolenghi, Proc. Natl. Acad. Sci. U.S.A. 76 (1979) 2503.

11 A. Warshel, Nature 260 (1976) 679.

12 R.R. Birge and L.M. Hubbard, J. Am. Chem. Soc. 102 (1980) 2195.

13 K. Peters, M.L. Applebury and P.M. Rentzepis, Proc. Natl. Acad. Sci. U.S.A. 74 (1977) 3119.

14 K. van der Meer, J.J.C. Mulder and J. Lugtenberg, Photochem. Photobiol. 24 (1976) 363.

15 A. Lewis, Proc. Natl. Acad. Sci. U.S.A. 75 (1978) 549.

16 A. Sarai, T. Kakitani and H. Kakitani, Photochem. Photobiol. 33 (1981) 875.

17 F.K. Fong, Theory of molecular relaxation (Wiley, New York, 1975) p. 75 (this reference contains a clear and detailed derivation of eq. 1).

18 D.J. Diestler, in: Radiationless processes in molecules and condensed phases, ed. F.K. Fong (Springer, Berlin, 1976) p. 169.

19 V.G. Levich, R.R. Dogonadze, E.D. German, A.M. Kuznetsov and Yu.I. Kharkats, Electrochim. Acta 15 (1970) 353.

20 S. Conte and C. deBoor, Elementary numerical analysis (McGraw-Hill, New York, 1980) p. 406.
21 N. Winter, D.J. Diestler and V. McCoy, J. Chem. Phys. 48 (1968) 1879.
22 B.G. Wicke and D.O. Harris, J. Chem. Phys. 64 (1976) 5236.
23 P.R. Bevington, Data reduction and error analysis for the physical sciences (McGraw-Hill, New York, 1969).
24 L.D. Landau and E.M. Lifshitz, Mechanics (Pergamon Press, Elmsford, New York, 1977).
25 K.C. Chou, Biophys. J. 45 (1984) 881.
26 B. Brooks and M. Karplus, Proc. Natl. Acad. Sci. U.S.A. 80 (1983) 6571.